Malaysian Journal of Analytical Sciences (MJAS)
Published by Malaysian Analytical Sciences Society

GEOPOLYMER FOAM REINFORCED NANOCELLULOSE PREPARED IN LOW MOLARITY ALKALINE SOLUTION: OPTIMISATION OF COMPRESSIVE STRENGTH

(Geopolimer Berliang Diperkukuh Dengan Nanoselulosa Disediakan Dalam Kepekatan Rendah Larutan Beralkali: Pengoptimuman Kekuatan Mampatan)

Chai Hua Tay[1,4], Norkhairunnisa Mazlan[2,3,4], Aimrun Wayayok[5], Mohd Salahuddin Mohd Basri[6], and Mohd Mustafa Albakri Abdullah[7]

[1]*Institute of Tropical Forestry and Forest Product, Universiti Putra Malaysia, 43400 Serdang, Selangor, Malaysia*
[2]*Department of Aerospace Engineering, Faculty of Engineering, Universiti Putra Malaysia, 43400 UPM Serdang, Selangor*
[3]*Institute of Nanoscience and Nanotechnology (ION2), Universiti Putra Malaysia, 43400 UPM Serdang, Selangor*
[4]*Aerospace Malaysia Research Center, Universiti Putra Malaysia, 43400 UPM Serdang, Selangor*
[5]*Department of Biological and Agriculture Engineering, Universiti Putra Malaysia, 43400 Serdang, Selangor, Malaysia*
[6]*Department of Process and Food Engineering, Universiti Putra Malaysia, 43400 Serdang, Selangor, Malaysia*
[7]*Construction Materials Engineering and Technology at Center of Excellence, Universiti Malaysia Perlis, 01000 Kangar, Perlis, Malaysia*

[*]*Corresponding author: norkhairunnisa@upm.edu.my*

Received: 11 November 2023; Accepted: 4 June 2024; Published: 29 December 2024

Abstract

In this work, Nanocellulose (NC) reinforced geopolymer foams are prepared in a low molarity potassium hydroxide (KOH) solution between 0.32M and 1.62M. Response Surface Methodology (RSM) is used to design experiments and optimise the compressive strength of the resulting geopolymer foam. The factors studied are seawater/potassium silicate (SW/KSil), potassium hydroxide/potassium chloride (KOH/KCl), sodium lauryl ether sulphate/benzalkonium chloride (SLES/BAC) and hydrogen peroxide/nanocellulose (H_2O_2/NC). The model adequacy checking revealed that the RSM model fits the data of this study well. All the factors are found to be significant with p <0.05. Surface plots revealed that in the low molarity environment, increasing the H_2O_2 content resulted in a steady decrement of compressive strength of geopolymer foam by 88%. In the geopolymer slurry stabilised with BAC, increasing the KOH concentration improved the compressive strength by up to 60%. On the other hand, in the geopolymer slurry stabilised with SLES, increasing KOH concentration resulted in decreasing compressive strength up to 50%. Higher formation of geopolymer nanogel is detected from the microscopical images at higher KOH concentration. The presence of geopolymer adhesion on the surface of NC was also presented. The predicted optimum compressive strength was 0.69 MPa. In conclusion, an optimisation of the composition for the geopolymer foam was conducted to achieve an optimum compressive strength which subsequently placed the produced foams comparable to Class I of low strength concrete for insulation and void filler applications.

Keywords: Response surface methodology, geopolymer foam, nanocellulose, compressive strength, optimisation

Abstrak

Dalam kerja ini, geopolimer berliang yang diperkuatkan dengan nanoselulosa disediakan dalam larutan kalium hidroksida (KOH) kemolaran rendah antara 0.32M hingga 1.62M. Metodologi Tindak Balas Permukaan (RSM) digunakan untuk mereka bentuk eksperimen dan mengoptimumkan kekuatan mampatan. Faktor yang dikaji ialah air laut/kalium silikat (SW/KSil), kalium hidroksida/kalium klorida (KOH/KCl), natrium lauril eter sulfat/benzalkonium klorida (SLES/BAC) dan hidrogen peroksida/nanoselulosa (H_2O_2/NC). Semakan kecukupan model mendedahkan bahawa model sesuai dengan data dengan baik dalam kajian ini. Kesemua faktor didapati signifikan dengan p <0.05. Plot permukaan mendedahkan bahawa dalam persekitaran kemolaran rendah, peningkatan kandungan H_2O_2 mengakibatkan penurunan kekuatan mampatan geopolimer berliang yang stabil sebanyak 88%. Dalam buburan geopolimer yang distabilkan oleh BAC, peningkatan kepekatan larutan KOH daripada 0.32M kepada 1.62M membawa kepada peningkatan kekuatan mampatan sebanyak 60%. Dalam buburan geopolymer yang distabilkan oleh SLES, penurunan kekuatan mampatan adalah sebanyak 50%. Imej mikroskopik mendedahkan kehadiran nanogel geopolimer dalam sampel geopolimer, dengan pembentukan yang lebih tinggi dalam kepekatan larutan KOH yang lebih tinggi. Terdapat juga kehadiran lekatan geopolimer pada permukaan NC. Kekuatan mampatan optimum yang diramalkan ialah 0.69MPa. Kekuatan mampatan yang dicapai meletakkan geopolimer berliang dalam jenis konkrit kekuatan rendah Kelas I, dengan potensi penggunaan sebagai bahan penebat dan pengisi lompang.

Kata kunci: Metodologi tindak balas permukaan, geopolymer berliang, nanoselulosa, kekuatan mampatan, pengoptimuman

Introduction

Geopolymer is an inorganic material prepared by dissolving aluminosilicates primarily in alkaline solution or somewhat less frequently in acidic solution. The dissolution forms networks of mineral molecules linked by covalent bonds [1]. Geopolymer is often regarded as a more environmentally friendly substitute for Ordinary Portland Cement (OPC) due to less CO_2 emissions during its preparation and its use of aluminosilicates that is commonly in waste and byproduct form [2]. However, geopolymer is not confined to concrete only as its application spans coating, adhesive, resin, and waste encapsulation [3]. This contributes to a high number of published research paper on geopolymers, up to almost 10,000 publications, which is equivalent to 1,200% increase from 2011 to 2022 [4]. This established the importance and rapid expansion of geopolymer research in the current era.

Despite numerous studies, there are concerns about the material supply, risks to human health, production cost and environmental impacts associated with geopolymer production, which limits widespread production and market acceptance. This is primarily due to the use of concentrated NaOH and KOH solution between 8M to 16M in geopolymer preparation [5-7]. According to Assi [8], approximately only 7% of OPC can be replaced by geopolymer prepared in 14M NaOH solution. This is due to the limited global supply of NaOH, causing the alkaline solution to be the most expensive component of the geopolymer mixture. Additionally, the KOH concentration of more than 1.78M is already considered corrosive to humans [9], indicating that the preparation of geopolymers requires the extensive use of Personal Protective Equipment (PPE) such as chemical-resistant gloves, safety glasses, and respirator which leads to higher costs in the production of geopolymers. Furthermore, according to GI Chemicals [10], the release of 4.45M of KOH solution into the soil induces toxicity to aquatic organisms.

Therefore, there is a need to prepare geopolymer in a low molarity alkaline solution, specifically in a KOH solution of less than 1.78M to mitigate the mentioned issues. This is supported by recent published work that has begun to fabricate geopolymer in low molarity alkaline solution as low as 1M [11], 1.5M [12] and 2M [13-18]. However, none of these works focus on the preparation of geopolymer foam in low molarity alkaline solution, which is equally important. While geopolymer form exhibits lower strength due to its porosity compared to geopolymer concrete, the porosity provides additional advantages for other applications such as lightweight concrete [19], thermal insulation [20], and waste removal [21]. This leads to a research gap in the preparation and characterisation of low molarity geopolymer foam in terms of compressive strength. In this study, RSM is used to design the experiment work consisting of four factors, namely seawater/potassium silicate (SW/KSil), potassium hydroxide/ potassium chloride (KOH/KCl), sodium lauryl ether sulphate/benzalkonium chloride

(SLES/BAC) and hydrogen peroxide/nanocellulose (H_2O_2/NC). The concentration range of KOH solution is kept low, between 0.32M to 1.62M. In the context of this study, the low molarity of the alkaline solution refers to the mentioned concentration. RSM is also used to determine statistically the significant factors for compressive strength in the low alkaline environment and conduct optimisation to achieve the highest compressive strength. Finally, morphological images were used to elucidate the microstructure of geopolymer foam prepared in low molarity alkaline solution.

Materials and Methods

Materials

Zeolite powder obtained from West Java, Indonesia, is sieved through 200 mesh openings to obtain finer particle size. Seawater is collected from Dataran 1 Malaysia, Melaka, Malaysia. KSil, KOH, and KCl were purchased from Sigma Aldrich. The elemental compositions of Zeolite and KSil are displayed in Table 1. Anionic SLES with 70% concentration is purchased from Evachem, cationic BAC with 80% concentration is purchased from Chemiz, and foaming agent H_2O_2 with 30% concentration purchased from R&M Chemicals. NC with width <50 nm and length >100 um, and concentration of 2.0 % (w/v) in distilled water was produced by ZoepNano.

Design of experiment using response surface methodology

RSM is conducted using Minitab software. Central Composite Design (CCD) experimental design method is chosen in this work as it is suitable to find the best possible product from ongoing batches in the process of optimisation [22]. The RSM used in this work consists of four factors and five levels as presented in Table 2. The factors used in this work are SW/KSil, KOH/KCl, SLES/BAC, and H_2O_2/NC. Two replications are chosen, with a total of 62 experimental runs and the value of α is two. Here, $\pm \alpha$ is the distance from the design centre to a star point where the distance from centre of the design space to a factorial point is ±1 unit for individual factor [23]. The levels are decided based on preliminary testing, which allows for workability during stirring and sample structure rigidity when immersed under water. The value for the total block is one, with the experiments conducted in a randomized order.

Table 1. Composition in zeolites and potassium silicate

Zeolite						
Chemical Composition	CaO	SiO_2	Fe_2O_3	Al_2O_3	K_2O	MgO
Concentration (%)	70.40	16.90	6.22	2.26	1.58	0.95
Potassium Silicate						
Chemical Composition		SiO_2			K_2O	
Concentration (%)		23.49			10.77	

Table 2. Factors and levels used in response surface methodology

Factors	**Unit**	**Wt.%**	**Notation**	**Levels**	
				Low	**High**
SW/KSil	g	-	V_1	1.05	1.15
KOH/KCl	%/%	10wt% of KSil	V_2	40/60	80/20
SLES/BAC	%/%	0.05wt% of Basic Geopolymer Slurry (BGS)	V_3	25/75	75/25
H_2O_2/NC	%/%	0.4wt% of BGS	V_4	25/75	75/25

Geopolymer foam formulation

Zeolite and KSil are kept at a constant ratio of 5:1. Therefore, a varying SW/KSil ratio is translated as constant KSil but a varying seawater content. The SW/KSil ratio is calculated based on their weight in grams. KOH/KCl is measured at 10 wt.% of KSil, resulting in a KOH solution with concentration ranging from 0.32M to 1.62M. When 10 wt.% of KSil correspond to 10g, a KOH/KCl ratio of 20/80 means that 2g of KOH and 8g of KCl are used. SLES/BAC is weighed with 0.05 wt.% of BGS while H_2O_2/NC is weighed with 0.4 wt.% of the BGS. The BGS consists

of zeolites, seawater, KSil, KOH and KCl. SLES/BAC and H_2O_2/NC ratios are calculated similarly to KOH/KCl.

Geopolymer foam fabrication

Figure 1 illustrates the processing route for preparation of geopolymer foam. The fabrication began with the dissolution of KOH and KCl pellets in seawater using a high shear stirrer. The solution is cooled to a room temperature of 30° C before KSil is added to produce the alkaline solution. Zeolite is then added to the alkaline solution, resulting in the solution called BGS. Subsequently, NC and BAC are added to BGS, followed by SLES and H_2O_2. Throughout the stirring process, the speed of high shear mixer is adjusted so that the formation of deep vortex is always formed to achieve optimum mixing, as suggested by Hockmeyer [24]. The geopolymer slurry is then poured into a silicone mould and cured at room temperature for one day before being removed from the mould. The samples are tested after 7 days.

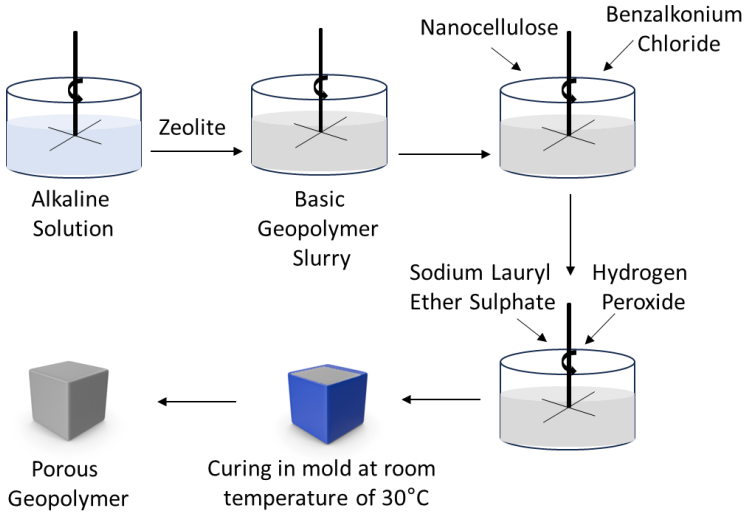

Figure 1. Processing route of geopolymer foam

Characterization

The compressive test is performed in accordance with ASTM D695 using an Instron Universal Testing Machine (UTM) with a load cell of 30kN. The compressive specimens are loaded at a rate of 1.3mm/min. The dimension of the specimens is 1cm x 1cm x 1.5cm. The morphological analysis is conducted using FEI NOVA NANOSEM230. The samples are first placed on an aluminium sample stub by using conductive carbon tape. The samples are then coated with platinum before being vacuumed in a sample chamber for observation.

Optimisation of geopolymer foam

An Analysis of Variance (ANOVA) is used to calculate the significance of factors and their interactions. A value of 95% is set as the confidence level, which corresponds to a ρ-value of 0.05. The model adequacy checking is conducted by analysing the normal probability plot, residual versus fitted value plot, histogram plot, and the versus order of the residual. The model adequacy checking is used to assess how well the fitted RSM model represents the measured data [25, 26]. Surface plot and contour plot are used to analyse the influence of the ratio of materials for each factor on the compressive strength of the fabricated geopolymer foam. Ultimately, an optimisation is performed to determine the best composition for highest compressive strength of the geopolymer foam. The optimised compressive strength is validated with actual experimental results.

Results and Discussion

Response surface methodology (RSM)

The complete design matrix and compressive strength values as well as the concentration of KOH solution with respect to each design matrix are shown in Appendix 1. Table 3 displays the ANOVA table

consisting of coefficient of determination (R^2) value for compressive strength. Equation 1 describes the regression model of the compressive strength as determined by RSM. Here, Y_{CS} is the regression model that estimate the compressive strength of the fabricated geopolymer foam based on the materials' composition (factors) as in Table 3 where SW/KSil is V_1, KOH/KCl is V_2, SLES/BAC is V_3, and H_2O_2/NC is V_4. The equation can be used to calculate and analyse the effect of factors on compressive strength of geopolymer foam. R^2 is always between 0% to 100%, and the higher the R^2 value, the better the compressive strength data fits the model. In this work, the R^2 value is nearing 100% with a value of 90.36% indicates that the regression model predicts the strength of the foamed geopolymer with good accuracy.

Table 3. ANOVA table for compressive strength

Model Summary				
R^2 = 90.36% R^2(adj)= 87.49%				
Term	**Notation**	**Coef.**	**SE. Coef.**	***p***
Constant		0.081005	0.006794	0
SW/KSil	V_1	-0.011182	0.003669	0.004
KOH/KCl	V_2	0.027446	0.003669	0
SLES/BAC	V_3	-0.026533	0.003669	0
H_2O_2/NC	V_4	-0.046918	0.003669	0
Square Term				
SW/KSil*SW/KSil	V_1*V_1	-0.006988	0.003361	0.043
KOH/KCl*KOH/KCl	V_2*V_2	0.006293	0.003361	0.067
SLES/BAC*SLES/BAC	V_3*V_3	0.007274	0.003361	0.036
H_2O_2/NC*H_2O_2/NC	V_4*V_4	0.008851	0.003361	0.011
Interaction Term				
SW/KSil*KOH/KCl	V_1*V_2	0.000685	0.004494	0.879
SW/KSil*SLES/BAC	V_1*V_3	0.008284	0.004494	0.072
SW/KSil*H_2O_2/NC	V_1*V_4	0.005478	0.004494	0.229
KOH/KCl*SLES/BAC	V_2*V_3	-0.02256	0.004494	0
KOH/KCl*H_2O_2/NC	V_2*V_4	-0.030361	0.004494	0
SLES/BAC*H_2O_2/NC	V_3*V_4	0.035934	0.004494	0

$$Y_{CS} = 0.081005 - 0.011182V_1 + 0.027446V_2 - 0.026533V_3 - 0.046918V_4 - 0.006988V_1V_1 + 0.006293V_2V_2 + 0.007274V_3V_3 + 0.008851V_4V_4 + 0.000685V_1V_2 + 0.008284V_1V_3 + 0.005478V_1V_4 - 0.02256V_2V_3 - 0.030361V_2V_4 + 0.035934V_3V_4 \quad (1)$$

Statistical analysis of compressive strength

Based on the ANOVA table in Table 3, the results showed that all four factors are highly significant with p value < 0.05, especially KOH/KCl, SLES/BAC, and H_2O_2/NC with a p value of 0. This implies that each factor significantly influences the compressive strength of the fabricated foamed geopolymer. Between the factors used in this work, H_2O_2/NC has the highest absolute coefficient value of 0.046918, indicating that the factor has the strongest effect on the compressive strength of geopolymer foam. On the other hand, SW/KSil has the least effect on the compressive strength with lowest absolute coefficient value of 0.011182, which tallies with its least significance p value of 0.004. The obtained results implied that all the factors highly influence the compressive strength of the foamed geopolymer. However, within the four factors presented, the changes in SW/KSil provided the least influence on compressive strength.

Model adequacy checking

Figure 2 displays the residual plots for compressive strength. The normal probability plot of the residuals in Figure 2(a) is approximately scattered along the straight line. This verifies the good assumption that the residuals are normally distributed. Patterns in the

normal probability plot that would violate the assumption of a normal distribution of the residuals are the observations of s-curve, inverted s-curve, downward curve, and a few points lying away from line, all of which are missing in the plot.

The graph of residual versus fits values in Figure 2(b) shows that the points generally fall randomly on both sides of zero, with no recognisable pattern in the points. This indicates that the residuals are randomly distributed and have a constant variance. Patterns that indicate that the model does not fulfil the model assumptions are the presence of many outliers and the fanning out or widening of the scatter among residuals with increasing value of the fits, which are not observed here. The histogram in Figure 2(c) shows a clear centre where most of the data cluster and has approximate bell shape, indicating a normal distribution. There is no clear indication of a long tail in one direction or many bars that are far away from other bars, which could indicate that the model does not fulfil the model assumptions.

Finally, the residual versus order plot in Figure 2d) displays that the residuals fall randomly around the centre line, confirming the assumption that the residuals are independent of each other. No increasing or decreasing trends, shifts, or cycles can be observed that could indicate that the residuals are interdependent [27]. Thus, these observations validate that the model is suitable for representing the variation in the data.

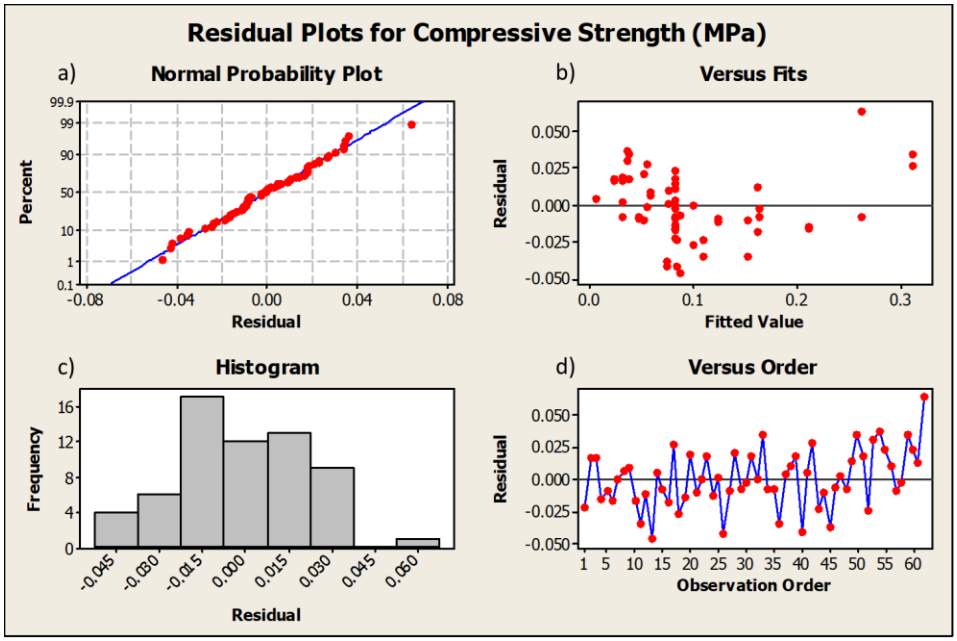

Figure 2. Residual plots

Surface plot and contour plot of compressive strength

Referring to Figure 3(a), Figure 3(b), and Figure (3c), the surface plots show the low compressive strength at high H_2O_2 ratio. This significant decrease in compressive strength with increasing H_2O_2 is consistent with the high absolute coefficient value of H_2O_2/NC, as shown in the ANOVA table (Table 3). As a foaming agent, the presence of high H_2O_2 is expected to induce high porosity in the geopolymer structure. This high porosity then leads to low compressive strength. For example, as in Figure 3(b), with a ratio of SW/KSil of 1.1, SLES/BAC of 50/50 and KOH/KCl of 100/0, an increase in H_2O_2 content from 0wt% to 0.4wt% of BGS showed a huge decrement in compressive strength by 88%, from higher than 0.4MPa to less than 0.05MPa.

The same observation is reported by Acar [28] in perlite-based-aerated geopolymer using H_2O_2, prepared in 16M NaOH solution. When the H_2O_2 amount is increased from 0.25wt% to 1wt% of the mass of the perlite, the compressive strength of the aerated

geopolymer decreases steadily by 75%, from 4MPa to 1MPa. This shows that, regardless of the concentration of the alkaline solution, an increase in H_2O_2 content leads to increased foaming reaction, which results in lower compressive strength. However, it is important to note that the decomposition rate of H_2O_2 is greater at higher concentration of alkaline solution [29, 30]. Therefore, it is important to control the amount of H_2O_2 introduced into the geopolymer foam depending on the concentration of the alkaline solution to achieve the desired compressive strength. At the same time, the dissolution of aluminosilicate is lower in a low concentration alkaline solution. Thus, a lower compressive strength is expected in this study compared to other studies in which concentrated alkaline solution were used in geopolymer preparation.

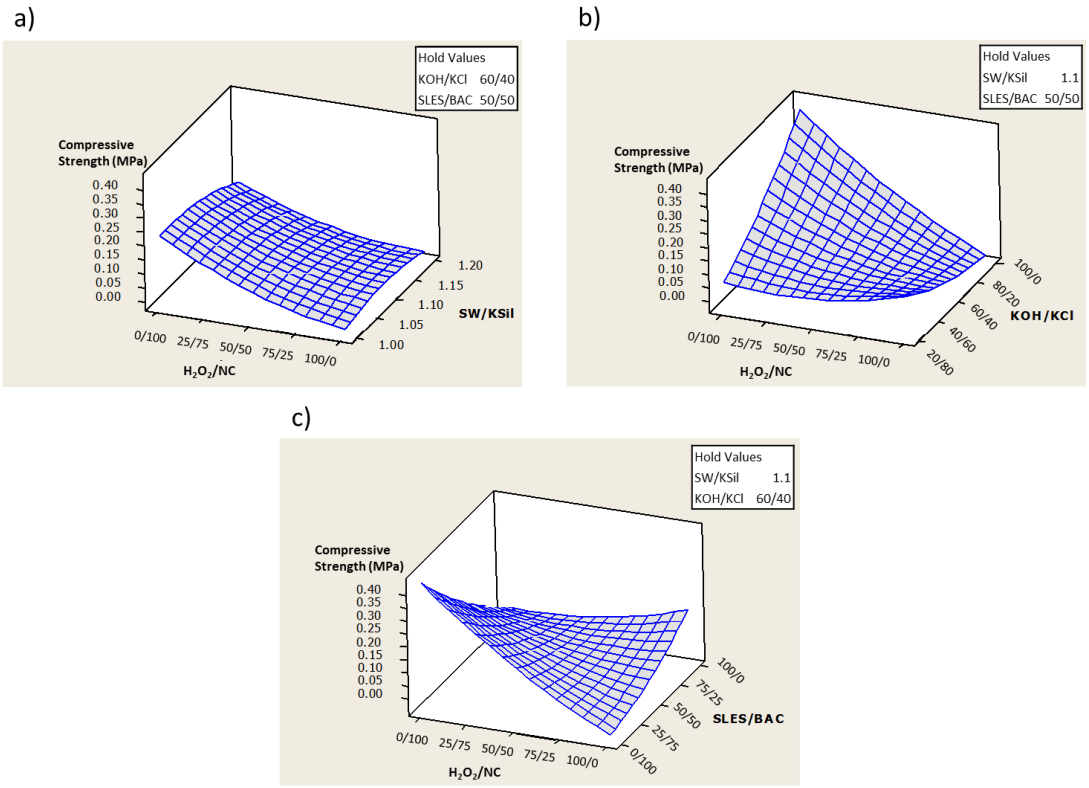

Figure 3. Compressive strength surface plot with H_2O_2/NC versus a) SW/KSil, b) KOH/KCl and c) SLES/BAC

Figure 4 depicts the contour plot of the compressive strength. Figure 4(a) shows that in an environment with hold values of SLES/BAC and H_2O_2/NC at 50/50, at high SW/KSil ratio and low KOH concentration, the compressive strength is low. Reducing the SW/KSil and increasing the KOH/KCl ratios improved the compressive strength. At SW/KSil of 1.05 and KOH/KCl of 100/0, the composition produced the highest compressive strength within 0.15-2.0MPa. This is due to the lower seawater content and higher KOH content, producing a more concentrated alkaline solution. Thus, more zeolite is dissolved which increases the compressive strength. This indicates that even for low molarity geopolymer foam, the change in alkaline solution concentration caused by varying water content is a crucial factor that affects the compressive strength.

Figure 4(b) illustrates the contour plot of two types of surfactants, SLES and BAC against KOH/KCl ratio where SW/KSil and H_2O_2/NC ratio are maintained at 1.1 and 50/50, respectively. In the presence of 100% BAC, the highest KOH/KCl ratio produces the highest compressive strength. On the other hand, when using 100% SLES, an increasing concentration of KOH solution leads to a decrease compressive strength, especially from 80% KOH to 100% KOH, where the compressive strength drops to less than 0.05MPa. Similar observation was made by Yan [31], where the use of BAC leads to a lower porosity and more

compact structure, resulting in a higher compressive strength compared to sodium lauryl sulphate (SLS) (similar formula to SLES). This is because BAC has a stronger adsorption capacity that binds itself to negatively charged Metakaolin. Zeolites, which are also negatively charged particles [32], benefits from the same mechanism when they come into contact with a cationic surfactant such as BAC. This leads to steric repulsion between the grains, which is beneficial for the dispersion of the zeolite particles [33]. This can efficiently promote the dissolution of zeolite and therefore increase the formation of geopolymer binders, resulting in a denser structure [34]. Thus, with the aid of higher concentration of KOH solution, the repulsion between BAC and zeolite promotes even greater dissolution that resulted in higher compressive strength.

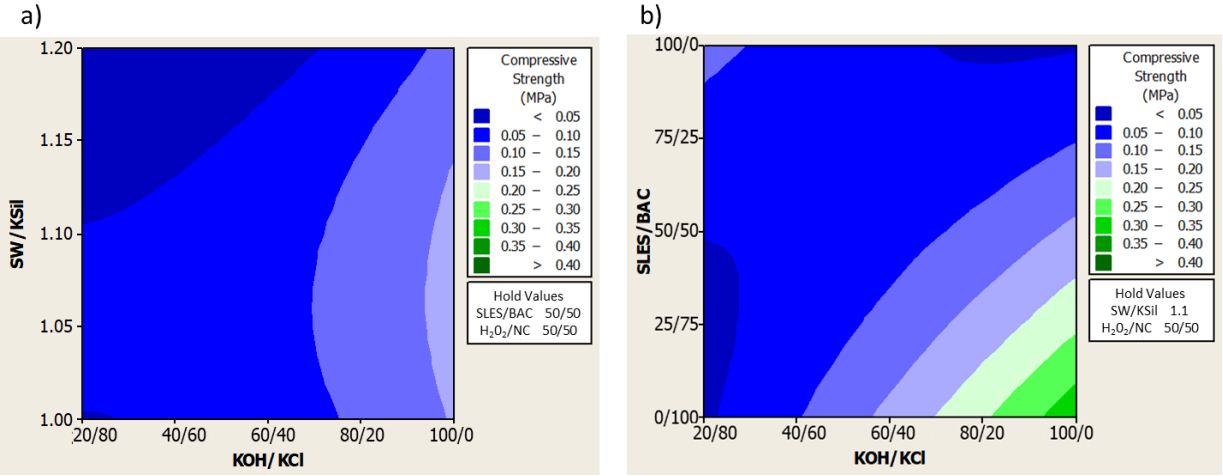

Figure 4. Compressive strength contour plot with KOH/KCl versus a) SW/KSil and b) SLES/BAC

Microscopical analysis on low molarity geopolymer foam

Figure 5 shows the microscopical image of zeolite and fabricated geopolymer samples at increasing concentrations KOH solution. In Figure 5(a), the zeolite illustrates the irregular shapes with the presence of fibrous, long structure, which is similar with the natural zeolite, as reported by Minceva et al. [35]. In Figure 5(b) which displays the geopolymer foam prepared in 0.32M of KOH solution, it can be noticed that there is the presence of unreacted fibrous zeolite. On the other hand, in Figure 5(c) and 5(d), there are less unreacted zeolite observed as the concentration of KOH solution increases, indicating that the higher concentration of KOH solution at 0.89M and 1.62M can dissolve the zeolite better. This is a common observation for geopolymer material prepared in high concentration of alkaline solution, particularly at the increasing of 2M to 8M of NaOH solution [36] and at the increasing of 3M to 12M of KOH solution [37]. However, such observation has not been reported before for geopolymer that is prepared in KOH solution below 2M, except for this study. Therefore, these observations indicated that within the range of KOH solution concentration between 0.32M to 1.62M, the difference in dissolution rate of zeolite is distinctive. This information would be useful for geopolymer studies focusing on the preparation in low molarity media.

Additionally, the presence of numerous geopolymer nanogel can be observed in Figure 5(d). According to Kriven [38], this is the intrinsic microstructure of geopolymer, which is a meshwork of polyciliate beads, each approximately 20nm in diameter, as displayed in Figure 6. This formation of nanogel was observed in the clay-based geopolymer prepared in 6M to 10M alkaline solution prepared by Kriven [38]. In this study, these geopolymer nanogel are also observed for samples that prepared at 0.32M and 0.89M, however the formation is relatively lower. Nevertheless, this validates that geopolymerisation has occurred in all the geopolymer samples prepared in low molarity KOH solution. This may be due to the optimum stirring of geopolymer slurry using a high shear mixer.

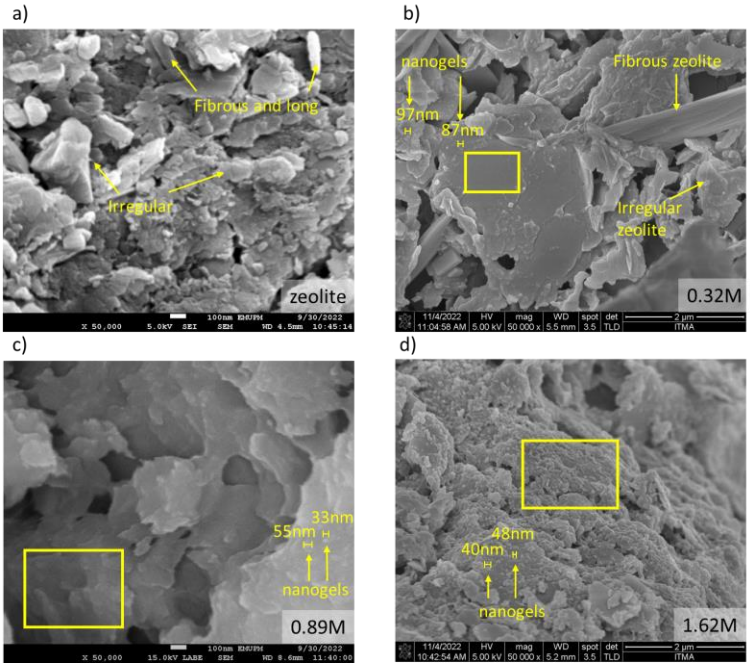

Figure 5. Microscopical images of a) Zeolite, and geopolymer samples fabricated in b) 0.32M, c) 0.89M and d) 1.62M KOH solution

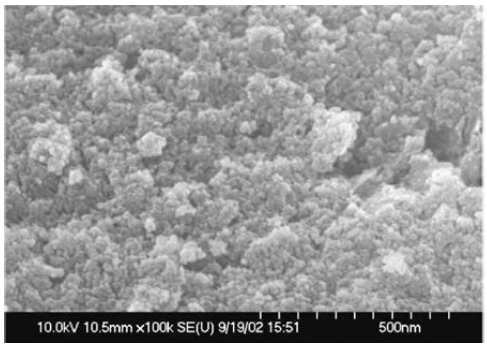

Figure 6. Microscopical image of fully reacted geopolymer [36]

Figure 7 shows the microscopical images of S26 geopolymer sample that is reinforced with 0.3wt% of NC. Referring to Figure 7(a), it can be observed that there is the presence of geopolymers adhered to the NC. A clearer view of the adhesion is in Figure 7(b), which indicates that there is strong interfacial adhesion between the NC with geopolymer matrix, as supported by other published work [39], contributing to high compressive strength. Figure 7(a) also depicts the well distribution of NC in the geopolymer, as shown by short arrows. This highlights the formation of uniformly distributed NC skeleton network which improves load distribution, resulting in a higher compressive strength of the geopolymer material [40].

Optimisation of the compressive strength

An optimisation plot for compressive strength is shown in Figure 8. The aim is to optimise compressive strength. The calculated composite desirability is 1.0000, which proves that the parameters used are well within the experimental range. The optimized values are SW/KSil of 1.03, KOH/KCl of 90.30/9.70, SLES/BAC of 0/100 and H_2O_2/NC of 0/100, with a predicted compressive strength of 0.6916 MPa.

Experimental validation

Table 4 shows the experimental results of the optimised composition of geopolymer foam related with Figure 8 (SW/KSil of 1.03, KOH/KCl of 90.30/9.70, SLES/BAC of 0/100 and H_2O_2/NC of 0/100). Five

samples are tested and labelled as SV1 to SV5. The errors calculated for the compressive strength are between 1.92%-4.45%, averaging at 3.80%. This value is significantly lower than 15% which shows that the regression model used in this work can be used to optimise the compressive strength of the geopolymer foam, as mentioned by Basri [41]. As a geopolymer foam prepared in low molarity alkaline solution, its compressive strength is expected to be low. However, the compressive strength achieved is sufficient for the material to be categorized under Class 1, low strength concrete [42]. The material is important and versatile for use in modern construction [43]. The application of low strength geopolymer foam is not only used as an insulating material, but also has other engineering applications such as large-span bridges, high-rise buildings, tall concrete wind towers [44] and offshore oil platforms due to its lower density, higher strength/weight ratio and better durability properties [45].

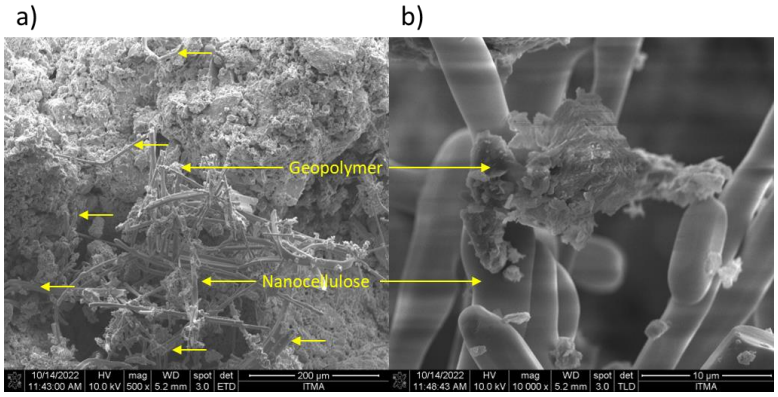

Figure 7. Microscopical images showing geopolymer adhesion onto NC at a) 500x and b) 10,000x magnification

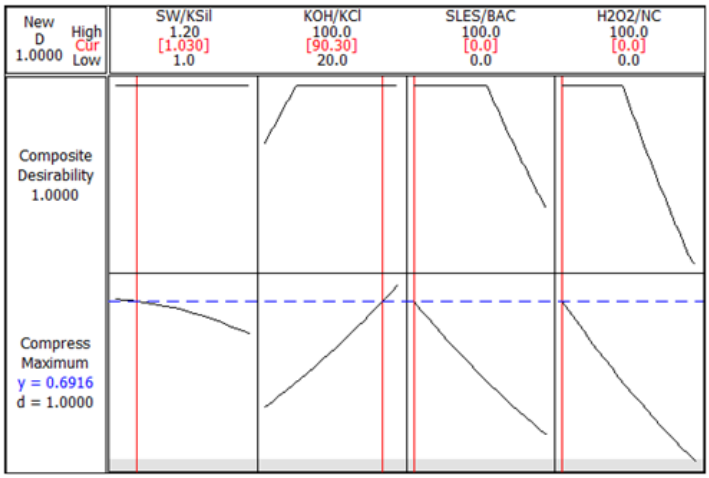

Figure 8. Optimisation plot of compressive strength.

Table 4. Experiment validation for compressive strength using the optimised geopolymer foam composition

Sample	Experimental Value (MPa)	Predicted Value (MPa)	Error (%)
SV1	0.71	0.69	1.92
SV2	0.67	0.69	3.81
SV3	0.66	0.69	4.37
SV4	0.66	0.69	4.44
SV5	0.72	0.69	4.45
Average	0.68	0.69	3.80

Additionally, the optimized sample produced can be used as a basis for further development for constructing concrete waterproofing in rocks with radioactive waste. This is due to the similar compressive strength of 0.5MPa after 2 days and 1.0MPa after 7 days [46]. The average compressive strength of 0.68MPa for the validation sample can be further developed to achieve a higher strength. The geopolymer foam can be used as a Controlled Low-Strength Materials (CLSM) or flowable slurry. It is a cementitious material primarily used for non-structural and light-structural applications, such as back-fills, sound insulating and isolation fills, pavement bases, conduit bedding, erosion control, and void filling. The compressive strength of the optimised geopolymer foam in this study is 0.68MPa, which is in a good agreement with that of CLSM produced by Naik [47] with 0.45MPa, 0.07MPa, and 0.38MPa on the same test day of 7th day after mixing the slurry.

Conclusion

Concentrated alkaline solution is the restricting factor which limits the widespread production and market adoption of geopolymer material. Therefore, in this study, geopolymer foam reinforced NC was prepared in a low molarity media of 0.32M to 1.62M KOH solution. RSM in conjunction with CCD were used to statistically analyse the effects of SW/KSil, KOH/KCl, SLES/BAC and H_2O_2/NC factors on compressive strength. The method is also used to optimise the compressive strength of the geopolymer foam. All the factors are found to be significant, with p value < 0.05. The expectation that the higher H_2O_2 content leads to lower compressive strength is found to be true for geopolymer samples prepared in low molarity alkaline solution. The presence of BAC promotes better dissolution of zeolite compared to anionic SLES due to the repulsion between cationic BAC and negatively charged zeolite. The ability of low molarity KOH solution to dissolve the zeolite and form a geopolymer nanogel can be contributed by the optimal stirring with a high shear mixer. The positive reinforcement of the NC in the geopolymer is reflected in the strong interfacial adhesion between the NC and geopolymer, as well as in the good distribution of the NC in the geopolymer binder, which contributes to a higher compressive strength. The compressive strength of the samples produced with the optimisation model is 0.68MPa on average and is therefore classified as Class 1 low strength concrete. Conclusively, this study reveals that geopolymer material can be prepared in low molarity alkaline solution, however exhibiting a low compressive strength. Further research can explore the use of other aluminosilicates such as metakaolin and slag, to make use of their low Si:Al ratio, as well as to incorporate aggregates, both to improve the compressive strength of the geopolymer material.

Acknowledgement

This project was supported by KPT under FRGS/1/2019/TK05/UPM/02/14. The authors declare no conflict of interest.

References

1. Davidovits, J. (2017). Geopolymers: Ceramic-like inorganic polymers. *Journal of Ceramic Science and Technology,* 8(3): 335-350.
2. Assi, L., Carter, K., Deaver, E. E., Anay, R., and Ziehl, P. (2018). Sustainable concrete: Building a greener future. *Journal of Cleaner Production*, 198: 1641-1651.
3. Davidovits, J. (2015). Geopolymer chemistry and applications. Geopolymer Institute, Saint Quentin: pp. 4-5.
4. Matsimbe, J., Dinka, M., Olukanni, D., and Musonda, I. (2022). A bibliometric analysis of research trends in geopolymer. *Materials,* 15(19): 6979.
5. Esparham, A., and Moradikhou, A. B. (2021). Factors influencing compressive strength of fly ash-based geopolymer concrete. *Journal of Civil Engineering,* 53(3): 21-31.
6. Aouan, B., Alehyen, S., Fadil, M., Alouani, M. E., Khabbazi, A., Atbir, A., and Taibi, M. H. (2021). Compressive strength optimization of metakaolin‐based geopolymer by central composite design. *Chemical Data Collections,* 31: 100636.
7. Khairudin, N. W. A., Yasir, M. S., Majid, A. B., Wahab, M. A., Marzukee, N., Paulus, W., Philip, E., Thanalecthumy, and Irwan, M. N. (2015). Immobilization of spent ion exchange resin from PUSPATI TRIGA reactor using fly ash-based geopolymer. *Malaysian Journal of Analytical Sciences,* 19(3): 472-480.
8. Assi, L. N., Carter, K., Deaver, E., and Ziehl, P. (2020). Review of availability of source materials

for geopolymer/sustainable concrete. *Journal of Cleaner Production*, 263: 121477.

9. National Center for Biotechnology Information (2024). Potassium Hydroxide. https://pubchem.ncbi.nlm.nih.gov/compound/Potassium-Hydroxide. [Access online 25 March 2024].
10. GI Chemicals (2006). Caustic Potash Liquid (All Grades). https://www.gichemicals.ie/assets/downloads/GI_Chem_SDS_KOH_50.pdf. [Access online 25 March 2024].
11. Sunarsih, E. S., As'ad, S., Sam, A. M., and Kristiawan, S. A. (2023). The effect of sodium hydroxide molarity on setting time, workability, and compressive strength of fly ash-slag-based geopolymer mortar. *In Journal of Physics: Conference Series* (Vol. 2556, No. 1, p. 012019). IOP Publishing.
12. Jithendra, C., and Elavenil, S. (2020). Effects of silica fume on workability and compressive strength properties of aluminosilicate based flowable geopolymer mortar under ambient curing. *Silicon,* 12(8): 1965-1974.
13. Sunarsih, E. S., As' ad, S., Sam, A. R. M., and Kristiawan, S. A. (2023b). Properties of fly ash-slag-based geopolymer concrete with low molarity sodium hydroxide. *Civil Engineering Journal,* 9(2): 318-392.
14. Qin, T. S., Lim, N. H. A. S., Jun, T. Z., and Ariffin, N. F. (2022). Effect of low molarity alkaline solution on the compressive strength of fly ash based geopolymer concrete. *International Journal of Sustainable Building Technology and Urban Development,* 13(2): 155-164.
15. Singh, A., Bhadauria, S. S., Thakare, A. A., Kumar, A., Mudgal, M., and Chaudhary, S. (2024). Durability assessment of mechanochemically activated geopolymer concrete with a low molarity alkali solution. *Case Studies in Construction Materials,* 20: e02715.
16. Farida, F. M., Kusumohadi, C. S., Wibisono, J. J., and Surahman, A. (2023). Water and steam curing types and three NaOH molarities effects due to fly ash based geopolymer concrete compressive strength study. *Journal of Engineering Science and Technology,* 18(1): 167-177.
17. Rohit, P., Gunneswara Rao, T. D., and Chandrasekhar, M. (2024). Effect of construction demolition waste as fine aggregate and NaOH molarity on strength and fracture parameters of slag based geopolymer mortars. *Journal of Engineering and Applied Science,* 71(1): 37.
18. Kuun Reddy, S. R., and Bala Murugan, S. (2020). Experimental and microstructural assessment of ternary blended geopolymer concrete with different Na_2SiO_3-to-NaOH volume ratios. *Innovative Infrastructure Solutions,* 5(1): 33.
19. Dhasindrakrishna, K., Pasupathy, K., Ramakrishnan, S., and Sanjayan, J. (2021). Progress, current thinking and challenges in geopolymer foam concrete technology. *Cement and Concrete Composites*, 116: 103886.
20. Łach, M. (2021). Geopolymer foams—Will they ever become a viable alternative to popular insulation materials?—A critical opinion. *Materials,* 14(13): 3568.
21. Petlitckaia, S., Barré, Y., Piallat, T., Grauby, O., Ferry, D., and Poulesquen, A. (2020). Functionalized geopolymer foams for cesium removal from liquid nuclear waste. *Journal of Cleaner Production*, 269: 122400.
22. Bhattacharya, S. (2021). Central composite design for response surface methodology and its application in pharmacy. In Response surface methodology in engineering science. IntechOpen.
23. Coman, G., and Bahrim, G. (2011). Optimization of xylanase production by Streptomyces sp. P12-137 using response surface methodology and central composite design. *Annals of microbiology,* 61: 773-779.
24. Hockmeyer, H. (2010). Practical guide to high-speed dispersion. https://www.pcimag.com/articles/90302-a-practical-guide-to-high-speed-dispersion. [Access online 25 March 2024].
25. Khan, A., Do, J., and Kim, D. (2017). Experimental optimization of high-strength self-compacting concrete based on D-optimal design. *Journal of Construction Engineering and Management,* 143(4): 04016108.
26. Mohd Fazli, A. A., Zakaria, S. K., Abd Rahman, N. I. N., Salleh, S. Z., Yusoff, A. H., Salleh, N. A., ... and Teo, P. T. (2020). Optimization of rice husk ash (RHA) as partial replacement of cementing material in structural ceramic composite concrete using response surface methodology (RSM)

statistical experimental design. *Journal of Ceramic Processing Research,* 21(6): 667-682.

27. Minitab (2024). Residual plots for fit regression model. https://support.minitab.com/en-us/minitab/help-and-how-to/statistical-modeling/regression/how-to/fit-regression-model/interpret-the-results/all-statistics-and-graphs/residual-plots/#normal-probability-plot-of-residuals. [Access online 25 March 2024].
28. Acar, M. C., Çelik, A. İ., Kayabaşı, R., Şener, A., Özdöner, N., and Özkılıç, Y. O. (2023). Production of perlite-based-aerated geopolymer using hydrogen peroxide as eco-friendly material for energy-efficient buildings. *Journal of Materials Research and Technology,* 24: 81-99.
29. Špalek, O., Balej, J., and Paseka, I. (1982). Kinetics of the decomposition of hydrogen peroxide in alkaline solutions. *Journal of the Chemical Society, Faraday Transactions 1: Physical Chemistry in Condensed Phases,* 78(8): 2349-2359.
30. Nicoll, W. D., and Smith, A. F. (1955). Stability of dilute alkaline solutions of hydrogen peroxide. *Industrial & Engineering Chemistry,* 47(12): 2548-2554.
31. Yan, D.-M., Ruan, S.-Q., Chen, S.-K., Liu, Y., Tian, Y., Wang, H.-L. and Ye, T.-N. (2021). Effects and mechanisms of surfactants on physical properties and microstructures of metakaolin-based geopolymer. *Journal of Zhejiang University Science A,* 22(2): 130-146.
32. Rhodes, C. J. (2010). Properties and applications of zeolites. *Science Progress,* 93(3): 223-284.
33. Flatt, R., and Schober, I. (2012). Superplasticizers and the rheology of concrete. In Understanding the rheology of concrete Woodhead publishing: pp. 144-208.
34. Saleh, T. A., Tuzen, M., and Sarı, A. (2018). Polyamide magnetic palygorskite for the simultaneous removal of Hg(II) and methyl mercury; with factorial design analysis. *Journal of Environmental Management*, 211: 323-333.
35. Minceva, M., Fajgar, R., Markovska, L., and Meshko, V. (2008). Comparative study of Zn^{2+}, Cd^{2+}, and Pb^{2+} removal from water solution using natural clinoptilolitic zeolite and commercial granulated activated carbon. Equilibrium of adsorption. *Separation Science and Technology,* 43(8): 2117-2143.
36. Ivanović, M. M., Kljajević, L. M., Gulicovski, J. J., Petković, M., Janković-Častvan, I., Bučevac, D., and Nenadović, S. S. (2020). The effect of the concentration of alkaline activator and aging time on the structure of metakaolin based geopolymer. *Science of Sintering,* 52(2): 219-229.
37. Sha, D., Pan, B., and Sun, Y. (2020). Investigation on mechanical properties and microstructure of coal-based synthetic natural gas slag (CSNGS) geopolymer. *Construction and Building Materials,* 259: 119793.
38. Kriven, W. M., Bell, J. L., and Gordon, M. (2003). Microstructure and microchemistry of fully-reacted geopolymers and geopolymer matrix composites. *Ceramic Transactions,* 153(1994): 227-250.
39. Sapiai, N., Jumahat, A., Manap, N., and Usoff, M. A. I. (2015). Effect of nanofillers dispersion on mechanical properties of clay/epoxy and silica/epoxy nanocomposites. *Journal Teknologi,* 76: 107-111.
40. Zheng, Y., Wang, Z., Wan, Z., Yang, X., Lin, F., Chen, Y., ... and Lu, B. (2023). Mechanochemical fabrication of geopolymer composites based on the reinforcement effect of microfibrillated cellulose. *Ceramics International,* 49(1): 503-511.
41. Mohd Basri, M. S. (2016). Development of rice husk ash-based geopolymer binder for fire resistant coating. [Doctoral dissertation, Universiti Putra Malaysia].
42. Tenza-Abril, A. J., Satorre-Cuerda, R., and Compañ-Rosique, P. (2019). Compressive strength classification of lightweight aggregate concrete using a support vector machine model. *WIT Transactions on Engineering Sciences,* 125: 173-183.
43. Jafari, S., and Mahini, S. S. (2017). Lightweight concrete design using gene expression programming. *Construction and Building Materials,* 139: 93-100.
44. Qin, Q., and Li, V. C. (2019). Development of lightweight engineered cementitious composite for durability enhancement of tall concrete wind towers. *Cement and Concrete Composites,* 96: 87-94.
45. Pla, C., Tenza-Abril, A. J., Valdes-Abellan, J., and Benavente, D. (2018). Influence of microstructure on fluid transport and mechanical properties in structural concrete produced with lightweight clay

aggregates. *Construction and Building Materials,* 171: 388-396.

46. Pusch, R., Warr, L., Grathoff, G., Purbakhtiar, A., Knutsson, S., and Ramqvist, G. (2014). A study on cement-poor concrete with talc for borehole sealing in rock hosting radioactive waste. *Comunicações Geológicas,* 101(1): 71-74.
47. Naik, T. R., Kraus, R. N., Siddique, R., and Chun, Y. M. (2004). Properties of controlled low-strength materials made with wood fly ash. *Journal of ASTM International,* 1(6): 1-10.